Available online at www.sciencedirect.com
ScienceDirect
Catalysis Today 116 (2006) 298–303
CATALYSIS TODAY
www.elsevier.com/locate/cattod

A basic assessment of the reactivity of Ni catalysts in the decomposition of methane for the production of "CO_x-free" hydrogen for fuel cells application

G. Bonura [a], O. Di Blasi [a], L. Spadaro [a], F. Arena [b], F. Frusteri [a,*]

[a] *Istituto CNR-ITAE "Nicola Giordano", Salita S. Lucia 39, I-98126 Messina, Italy*
[b] *Dipartimento di Chimica Industriale e Ingegneria dei Materiali, Università degli Studi di Messina, Salita Sperone 31, 98166 S. Agata, Messina, Italy*

Available online 27 June 2006

Abstract

The hydrogen production through the decomposition of methane into hydrogen and carbon on Ni supported catalysts followed by catalyst regeneration in oxidative atmosphere was evaluated. Typical temperature programmed catalytic reaction (TPCR) results revealed that the nature of the carrier slightly affects the onset temperature of CH_4 decomposition, while catalytic performance and regeneration capacity in O_2 or CO_2 streams depend on dispersion and morphology of the active phase. The "structure-sensitive" character of methane decomposition reaction has been confirmed. TEM analyses of the "spent" catalysts revealed that both "filamentous" and "encapsulating" carbon species were formed under isothermal conditions at 823 K, the last being responsible for catalyst deactivation.

Keywords: Nickel catalysts; Hydrogen production; Methane decomposition; Carbon deposition; Catalyst regeneration

1. Introduction

Hydrogen is the most suitable fuel for fuel cells. Currently, steam reforming, partial oxidation and auto-thermal reforming of hydrocarbons are the major routes for hydrogen generation, but all these methods produce a large amount of CO_x as by-products along with hydrogen. Hydrogen generated by these conventional methods can be utilized to feed a low temperature fuel cell only if CO is completely eliminated [1]. Indeed, for proton exchange membrane fuel cells (PEMFC) CO is a strong poison even when its concentration is very low (10 ppm), whereas for alkaline fuel cells (AFC), besides CO, ppm levels of CO_2 are also poison. Removal of CO_x to ppm levels from the hydrogen stream makes the process complex and expensive and the exploration of alternative routes for the direct pure hydrogen production with specific applications in fuel cells is desired [2].

An alternative route for pure H_2 production could be the hydrocarbon decomposition to hydrogen and carbon. In this reaction, formation of carbon oxides is avoided and the need for downstream reactions such as water–gas shift and selective oxidation is eliminated [3,4].

In addition to hydrogen as a major product, the hydrocarbon decomposition process produces a very valuable coproduct, the carbon nanotube (CNT), considered a novel promising material for various technological applications. In recent years, filaments and nanotubes of various types have been synthesized and textural and adsorptive properties of this material, as well as kinetics and thermodynamics of formation over different catalysts, have been studied [5–8].

The direct catalytic decomposition of hydrocarbon into hydrogen and carbon (1) followed by catalyst regeneration in oxidative atmosphere (2) could be also an alternative route to be followed [9]:

$$CH_4 \rightarrow C + 2H_2, \quad \Delta H^\circ = 75\,\text{kJ/mol} \tag{1}$$

$$C + O_2 \rightarrow CO_2, \quad \Delta H^\circ = -283\,\text{kJ/mol} \tag{2}$$

Transition metals such as Fe, Co and Ni are well known to be effective for methane decomposition into hydrogen and carbon nanofibers. The nickel-based catalysts are active at low temperatures and provide a higher yield of CNT per mass unit of the

* Corresponding author. Fax: +39 090 624247.
E-mail address: francesco.frusteri@itae.cnr.it (F. Frusteri).

0920-5861/$ – see front matter © 2006 Elsevier B.V. All rights reserved.
doi:10.1016/j.cattod.2006.05.075

active component. For this reason, the nickel metal-based catalysts seem to be the most attractive for the industrial use [5,8]. However, Ni catalysts drastically deactivate and for a continuous H_2 supplying a two-step system based on reaction and regeneration is required [10,11].

The present work deals with the preparation, characterisation and testing of Ni supported catalysts in the methane decomposition reaction, focusing the attention to gain an understanding of the effects of support and metal dispersion on the reaction kinetics, catalyst deactivation and rate of CNT growth. The regeneration by O_2 or CO_2 streams of spent catalysts has also been investigated.

2. Experimental

2.1. Catalyst preparation

Supported Ni catalysts were prepared by the incipient wetness method, using an aqueous solution of $Ni(NO_3)_2{\cdot}6H_2O$. After impregnation the catalysts were dried overnight at 373 K and then calcined at 673 K for 4 h in air. MgO (UBE Ind. Ltd.; SA_{BET}, 34 $m^2\,g^{-1}$), SiO_2 (Degussa Aerosil 200; SA_{BET}, 175 $m^2\,g^{-1}$), ZrO_2 (Degussa VP; SA_{BET}, 15 $m^2\,g^{-1}$) and γ-$LiAlO_2$ (IGT; SA_{BET}, 25 $m^2\,g^{-1}$) were utilized as carriers of Ni. A commercial steam reforming catalyst (''CRG-F'') was used as reference sample. All the catalysts were pressed (≈400 bar), crushed and sieved and the 40–70 mesh fraction was used for catalytic measurements.

2.2. Catalyst characterization

Ni loading was determined by *X-ray fluorescence analysis* (XRF), using a spectrometer BRUKER AXS-S4 Explorer. Samples were analysed at the solid state and Ni loading was calculated from emission value of Ni $K\alpha_1$ transition, $E = 7.471$ keV. The analytical composition of catalysts was expressed in weight percentage of Ni metal.

Surface area was measured by BET method using a Sorptomatic Carlo Erba instrument, while the amount of carbon deposited on catalysts was evaluated by elementary analysis using a CHSN—Carlo Erba instrument.

Hydrogen chemisorption data were obtained by using a conventional flow apparatus operating both in continuous and pulse mode [12]. Catalysts (0.05–0.1 g) were placed in a linear quartz micro-reactor (i.d. = 4 mm; $l = 200$ mm) and reduced in hydrogen flow (3.6 STP L h^{-1}) at 923 K. After the reduction treatment, the sample was cooled in flowing H_2 to room temperature, equilibrated for 30 min, and then further cooled by a dry ice foam; afterwards H_2 was shut off and the sample was purged with argon flow (3.6 STP L h^{-1}) for 10 min. After purging at 193 K, the desorption process was started heating the sample until 1073 K in the argon carrier flow, with a heating rate (β) of 10 °C min^{-1}. The desorption process was monitored and quantified by a thermal conductivity detector (TCD) connected to a HP 6890 gas chromatograph. Before the desorption run a calibration test was performed by injecting in the carrier gas a known amount of H_2 in order to obtain reliable quantitative measurements. Metal dispersion (D) was calculated from the following experimental ratio by assuming the chemisorption stoichiometry $H/Ni_{surf} = 1$:

$$D\,(\%) = \left(\frac{X_{H_2}}{X_{O_2}}\right) \times 100,$$

where X_{H_2} is the hydrogen uptake ($\mu mol\,g_{cat}^{-1}$) and X_{O_2} is the oxygen uptake ($\mu mol\,g_{cat}^{-1}$) at 773 K, which corresponds to the fraction (α) of NiO reduced to Ni° according to the following oxidation stoichiometry: $Ni^\circ + 1/2O_2 = NiO$. Metal surface area (MSA, $m_{Ni}^2\,g_{cat}^{-1}$) was calculated assuming a Ni site density of 6.5 $Å^2$/atom [13], while the Ni mean particle size (d_s) was derived from the equation:

$$d_s\,(Å) = \frac{101}{D\,(\%)}$$

as suggested by Bartholomew et al. [14].

Spent catalysts were studied using TGA/DSC and transmission electron microscopy (TEM) analysis. For TGA/DSC analysis 15–20 mg of sample were treated in air in a thermobalance (Netzsch STA 409), from 298 to 1273 K with a heating rate (β) of 10 °C min^{-1}. TEM observations were made by using a Philips CM12 instrument equipped with a high-resolution camera which allows acquisition and elaboration of TEM images. Specimens were prepared by ultrasonic dispersion of catalyst samples in isopropyl alcohol depositing a drop of suspension on carbon grid.

In Table 1 are summarized the results of physico-chemical characterisation of the supported Ni catalysts prepared according to the aforementioned procedures.

2.3. Experimental set-up

Catalyst testing was performed in a programmed temperature mode (TPCR) using a U shaped quartz reactor and a catalyst sample of ca. 0.05 g diluted (1/3) with same sized carborundum (SiC). Before reaction, the catalysts were reduced

Table 1
Physico-chemical properties of the Ni based catalysts

Sample	Carrier	Ni loading (wt%)	SA_{BET} ($m^2\,g^{-1}$)	MSA ($m^2\,g^{-1}$)	D (%)	d_s (nm)	α ($Ni^\circ/Ni_{tot.}$)
Ni/MgO	MgO	48.0	31.0	18.1	11.9	8.5	0.48
Ni/SiO_2	SiO_2	16.2	171.0	6.4	9.7	10.4	0.61
$Ni/LiAlO_2$	γ-$LiAlO_2$	16.5	22.3	4.0	5.7	17.8	0.64
Ni/ZrO_2	ZrO_2	55.0	8.5	2.4	1.1	94.0	0.61
CRG-F	–	60.0	198.0	28.0	7.5	13.5	0.94

"in situ" at 923 K for 1 h under flowing hydrogen and then cooled down to 473 K. All experiments were performed in the T range 473–923 K, with a heating rate (β) of 10 °C min^{-1} using mixtures, flowing at 60 STP cm^3 min^{-1}, of the following composition: 10% CH_4/He for the TPCR run; 10% O_2/He for the first regeneration step (TPO), 10% CO_2/He for the second regeneration step (TPG) and 5% H_2/Ar for the reduction of the regenerated samples (TPR). The experiments were performed at atmospheric pressure and the pressure drop across the catalyst bed was negligible. CH_4 decomposition patterns were recorded by a Quadrupole Mass Spectrometer ('Thermolab', Fisons Instruments) connected on-line to the reactor by a heated (≈180 °C) inlet capillary system (transit time < 0.5 s). Mass spectra consisting of the following m/z signals: 4 (He), 16 (CH_4) and 2 (H_2) were collected in multiple ion monitoring (MIM) mode using the SEM amplifier operating at 2000 V and an ionization potential of −70 V (scan frequency, 2 s^{-1}). For the regeneration of catalysts, mass spectra of 4 (He), 32 (O_2), 28 (CO), 44 (CO_2) and 17 (OH) were considered in the conditions as above.

Furthermore, in order to evaluate the catalyst stability, experiments in isothermal conditions at 823 K were also carried out.

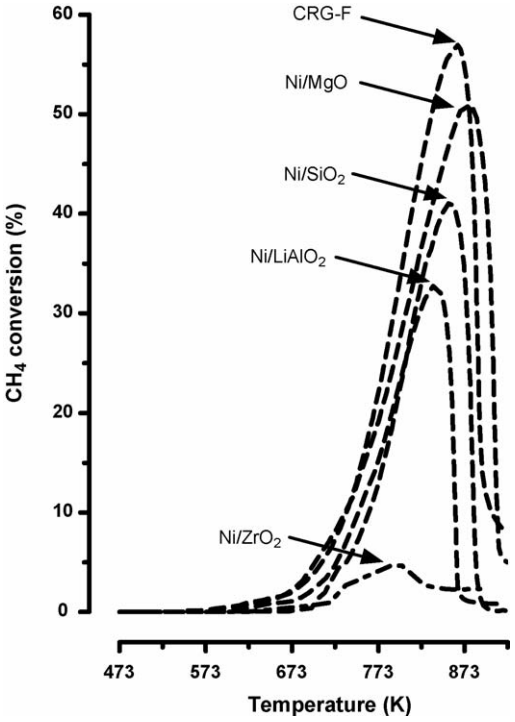

Fig. 1. Temperature programmed reaction of CH_4 (TPCR) over Ni supported catalysts.

3. Results and discussion

Although the unsteady-state regime of the temperature programmed measurements entails the formation of several species of carbonaceous deposits [3–8] not allowing for a quantitative comparison of the catalyst performance, such tests provide some preliminary information on the relative capability of the various systems to drive the methane decomposition before undergoing deactivation by coking.

Typical TPCR results are represented in Fig. 1. The CH_4 conversion gradually increases with the increasing of temperature until a maximum of conversion is reached, afterwards the CH_4 conversion drastically decreases as a consequence of catalyst deactivation. Only H_2 was obtained as a gaseous product in the reaction over all the investigated catalysts. The results shown in the figure clearly indicates that only slight difference in terms of on-set CH_4 decomposition temperature exists since hydrogen begins to form at about 603 K over all catalysts. On the contrary significant differences have been observed in terms of catalyst activity according to the following reactivity scale:

$$\text{CRG-F} > \text{Ni/MgO} > \text{Ni/SiO}_2 > \text{Ni/LiAlO}_2 > \text{Ni/ZrO}_2$$

Since the on-set temperature is similar on all catalysts investigated, methane activation should not be affected by the nature of support, even if should be considered that the support effect could be masked since the Ni particle size distribution changes from one catalyst to another and in any case Ni particles larger than 9 nm are present, then the metal–support interaction could be enough weak [15–17].

Catalytic data obtained in isothermal conditions are shown in Fig. 2. The Ni/MgO, Ni/SiO_2, $Ni/LiAlO_2$ systems achieve at

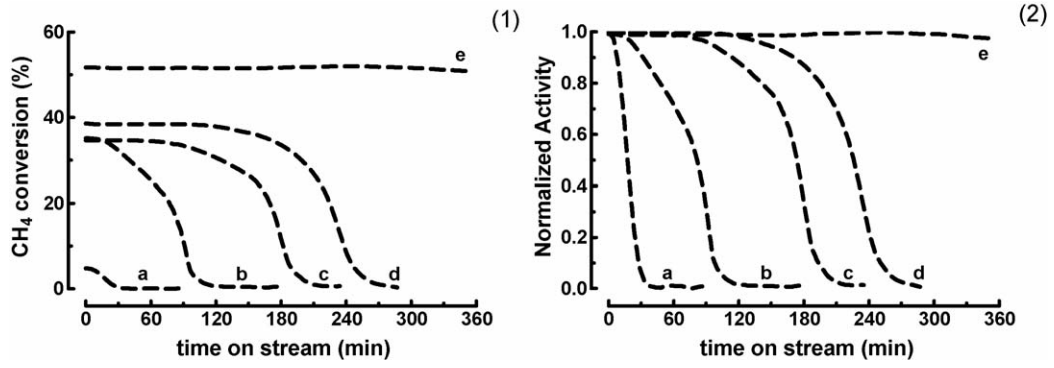

Fig. 2. Methane decomposition in isothermal conditions at 823 K and GHSV = 72,000 h^{-1}: (1) CH_4 conversion vs. time on stream; (2) normalized activity vs. time on stream. Pattern: (a) Ni/ZrO_2; (b) $Ni/LiAlO_2$; (c) Ni/SiO_2; (d) Ni/MgO; (e) CRG-F.

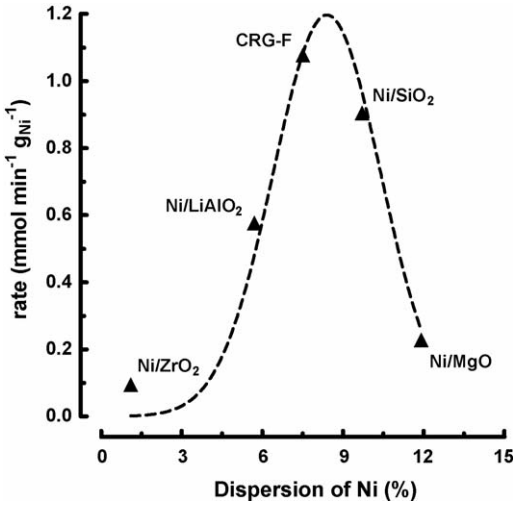

Fig. 3. Methane decomposition in isothermal conditions, reaction rate as a function of Ni dispersion.

823 K an initial conversion of methane approximately of 35–40%, while Ni/ZrO_2 presents a very low activity (5%). All catalysts deactivate but with a different trend. In general, CH_4 conversion remain constant in the first step of reaction till begins to decrease up to collapse just before the total catalyst deactivation. The systems with a greater MSA are more stable resulting thus in a longer lifetime, in particular the reference system CRG-F, with the highest MSA (28 $m^2_{Ni}\,g^{-1}_{cat}$), does not deactivate even after 360 min of time on stream.

In the attempt to rationalize the catalytic patterns, TPCR results have been normalized in terms of MSA. The reaction rate was calculated at conversion level close to 5% for all catalysts investigated. The typical volcano-shaped relationship obtained (see Fig. 3) by correlating the reaction rate (expressed as mmol of H_2 produced per min per gram of Ni) to the dispersion of the active phase of the catalysts, indicate how critical is the role of the metal dispersion on the catalyst performance, stressing thus the *structure-sensitive* character of CH_4 decomposition reaction. Similar volcano trend, recently observed for Ni/SiO_2 catalyst [16], was justified suggesting that a fundamental role in the kinetic of coke formation is played by the Ni particle size concluding that the catalyst deactivation and the CNT growth rates depend upon several factors like diffusion flux area, diffusion length, driving force of carbon diffusion and saturation concentration of CNT. The reduced coking rate on small size Ni crystal is a result of increased saturation concentration of CNT which leads to a low driving force of carbon diffusion and then a lower coking rate and a drastic deactivation; on the contrary in case of large Ni particles the formation of surface carbon from elementary reaction steps could become the rate determing step.

As regard the regeneration facility, Fig. 4 displays that the regeneration steps in O_2 (TPO) or CO_2 (TPG) allow an effective gasification of the carbonaceous deposits. However, a significant difference was observed in terms of on-set temperature, in fact in O_2 stream CO_2 starts to form at 630 K, while in CO_2 stream the on-set temperature was shifted at 740 K, and in any case a complete removing of coke was not reached up to 923 K [10].

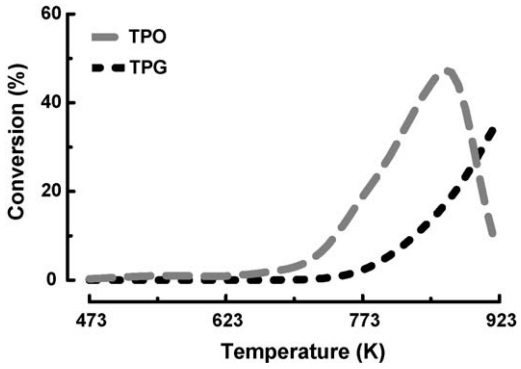

Fig. 4. TPO and TPG regeneration tests on Ni/MgO catalyst.

Regeneration tests carried out by reaction–oxidation–reduction cycles are shown in Fig. 5. It can be observed that the Ni/MgO catalyst performance is not significantly affected by regeneration cycles since neither the on-set temperature nor the methane conversion profile change with cycles. However, even if the result can be worthy of consideration, additional cycles should be carried out to demonstrate the real feasibility of process.

Regeneration tests performed without further reduction step (see Fig. 6) have demonstrated that the decomposition of methane occurs also on the NiO surface. CH_4 firstly reduces NiO to Ni° giving rise to the formation of H_2O and H_2,

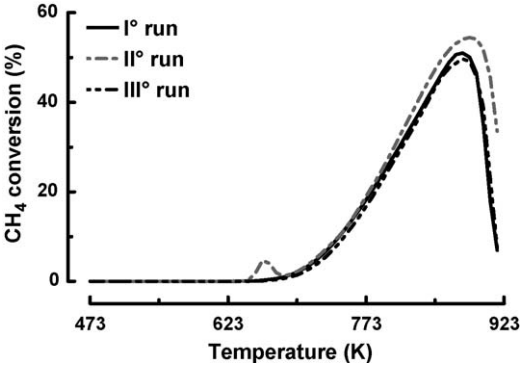

Fig. 5. Reaction cycles performed on Ni/MgO catalysts. I° run: "fresh" catalyst; II° run: after O_2-TPO; III° run: after CO_2-TPG. All runs were carried out after previous in situ H_2 reduction.

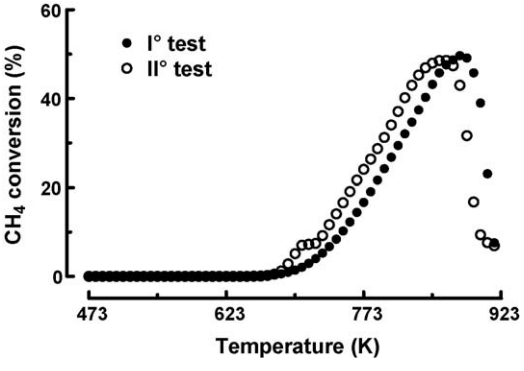

Fig. 6. II° run of TPCR on Ni/MgO catalysts. I° test: after O_2-TPO and subsequent in situ H_2-TPR; II° test: after O_2-TPO without further reduction.

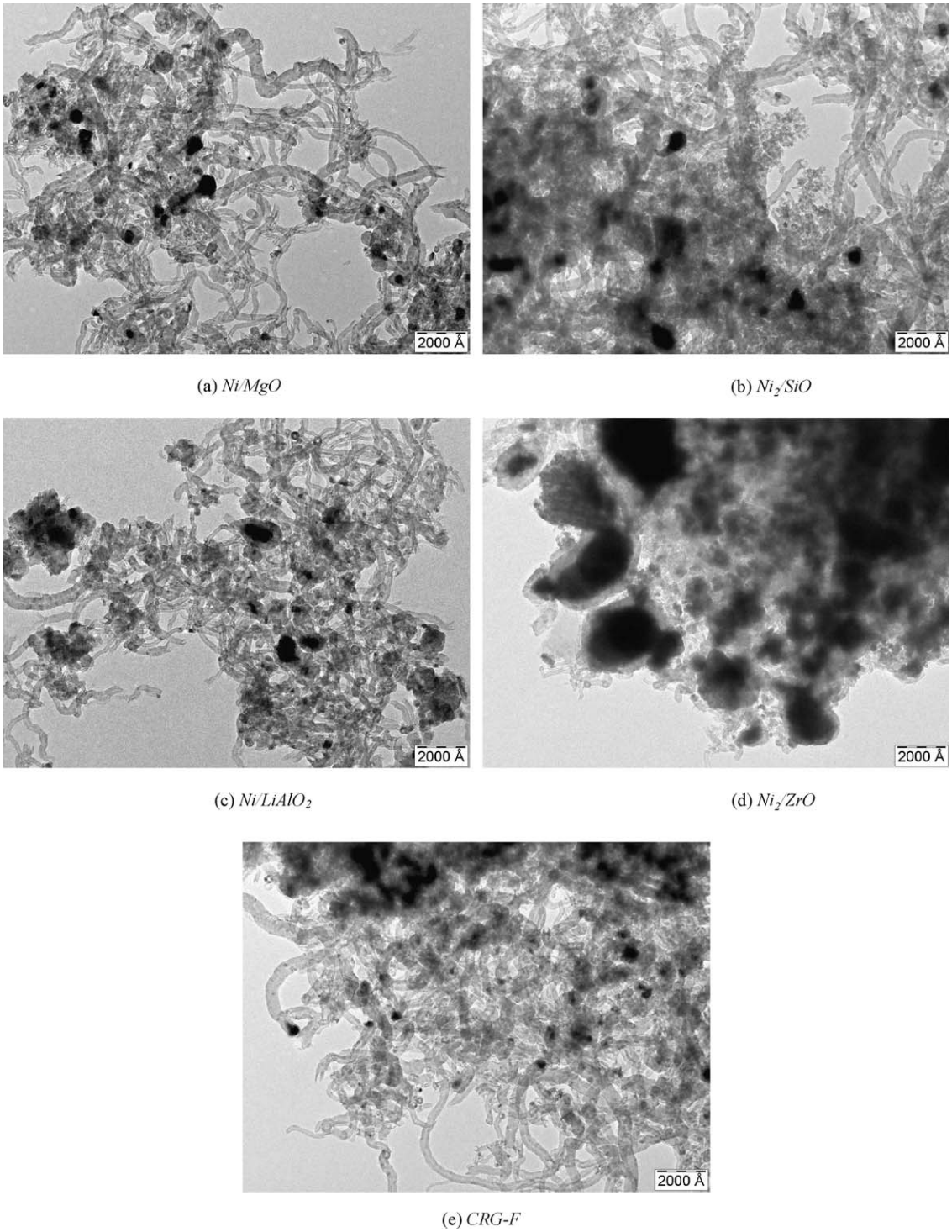

(a) *Ni/MgO* (b) *Ni_2/SiO*

(c) *Ni/$LiAlO_2$* (d) *Ni_2/ZrO*

(e) *CRG-F*

Fig. 7. TEM images of catalysts used in isothermal conditions.

afterwards it decomposes on reduced Ni into C and H_2. Only a slight difference in terms of on-set temperature being observed.

TEM investigation of spent catalysts revealed that both filamentous (*whiskers-shaped*) and condensed (*encapsulating-shaped*) carbon species were formed under isothermal conditions at 823 K (see Fig. 7). From the images it clearly emerges that the most active catalysts (Ni/MgO, Ni/SiO_2 and CRG-F) mainly promote the formation of filamentous carbon, while Ni/$LiAlO_2$ and Ni/ZrO_2 catalysts, characterized by larger particle diameter (>90 nm) promote the formation of encapsulated carbon responsible of the rapid deactivation of Ni particles.

The amount of coke formed during reaction was evaluated by TGA/DSC analysis. From the results shown in Fig. 8 it was confirmed that the highest carbon capacity is ensured for the systems characterized by Ni particles of 8–15 nm.

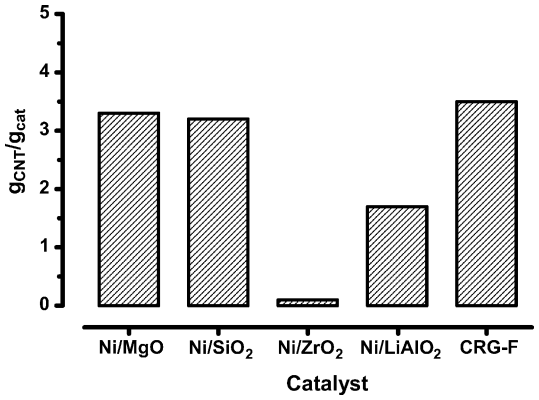

Fig. 8. Thermal analysis data: carbon yield (g_{CNT}/g_{cat}) on different catalysts.

4. Conclusions

On the basis of the above results described we conclude as follows:

- Ni supported catalysts show activity in the catalytic decomposition of CH_4 in the range of temperature 700–923 K. Typical TPCR results display that the nature of the carrier only slightly affecting the onset temperature of CH_4 decomposition.
- Catalytic performance and regeneration capacity in O_2 or CO_2 stream depend on the Ni dispersion and on the morphology of the active phase. The ''structure-sensitive'' character of methane decomposition reaction was demonstrated.
- The regeneration cycles allow an effective gasification of the carbonaceous deposits restoring the initial activity of the systems without any further reduction of NiO formed in the regeneration step.
- TEM analyses of the ''spent'' catalysts reveal that both ''whiskers'' and ''encapsulating'' carbon species are formed under isothermal conditions at 823 K. Small Ni particles mainly promote the formation of filamentous carbon.
- The main cause of the catalyst deactivation was ascribed to the incorporation of Ni particles into carbon shells, whereas negligible is the contribution of thermal sintering.

References

[1] T.V. Choudhary, D.W. Goodman, Catal. Today 77 (2002) 65–78.
[2] J. Chen, Y. Li, Z. Li, X. Zhang, Appl. Catal. A: Gen. 269 (2004) 179–186.
[3] T. Zhang, M.D. Amiridis, Appl. Catal. A: Gen. 167 (1998) 161–172.
[4] M. Steinberg, H.C. Cheng, Int. J. Hydrogen Energy 14 (1989) 797–820.
[5] M.A. Ermakova, D.Yu. Ermakov, G.G. Kuvshinov, L.M. Plyasova, J. Catal. 187 (1999) 77–84.
[6] M.A. Ermakova, D.Yu. Ermakov, G.G. Kuvshinov, Appl. Catal. A: Gen. 201 (2000) 61–70.
[7] N. Muradov, Int. J. Hydrogen Energy 26 (2001) 1165–1175.
[8] H.Y. Wang, E. Ruckenstein, Carbon 40 (2002) 1911–1917.
[9] B. Monnerat, L. Kiwi-Minsker, A. Renken, Chem. Eng. Sci. 56 (2001) 633–639.
[10] S. Takenaka, E. Kato, Y. Tomikubo, K. Otsuka, J. Catal. 219 (2003) 176–185.
[11] R. Aiello, et al. Appl. Catal. A: Gen. 192 (2000) 227–234.
[12] R.D. Jones, C.H. Bartholomew, Appl. Catal. 39 (1988) 77.
[13] J.S. Smith, P.A. Thrower, M.A. Vannice, J. Catal. 68 (1981) 270.
[14] C.H. Bartholomew, R.B. Pannell, J.L. Butler, J. Catal. 65 (1980) 335.
[15] R.L. Vander Wal, et al. Carbon 39 (2001) 2277–2289.
[16] De Chen, et al. J. Catal. 229 (2005) 82–96.
[17] S. Takenaka, et al. Appl. Catal. A: Gen. 217 (2001) 101–110.